Journal of Biomechanics 49 (2016) 216–221

Contents lists available at ScienceDirect

Journal of Biomechanics

journal homepage: www.elsevier.com/locate/jbiomech
www.JBiomech.com

Morphologic and biomechanical comparison of spinous processes and ligaments from scoliotic and kyphotic patients

Brian P. Beaubien [a,*], Andrew L. Freeman [a], Glenn R. Buttermann [b]

[a] Excelen Center for Bone and Joint Research and Education, 700 10th Avenue South, Minneapolis, MN 55415, United States
[b] Midwest Spine & Brain Institute, 1950 Curve Crest Boulevard, Stillwater, MN 55082, United States

ARTICLE INFO

Article history:
Accepted 3 December 2015

Keywords:
Ligament
Kyphosis
Material Properties
Scoliosis

ABSTRACT

The spinous processes and supraspinous and interspinous ligaments (SSL and ISL, respectively) limit flexion and may relate to spinal curvature. Spinous process angles and mechanical properties of explanted human thoracic posterior SSL/ISL complexes were compared for scoliosis ($n=14$) *vs.* kyphosis ($n=8$) patients. The median thoracic coronal Cobb angle for scoliosis patients was 48°, and sagittal angles for kyphosis patients was 78°. Spinous processes were gripped and four strain steps of 4% were applied and held. Percent relaxation was calculated over each step, equilibrium load data were fit to an exponential equation, and a Kelvin model was fit to the load from all four curves. Failure testing was also performed. Median ligament complex dimensions from scoliosis and kyphosis patients were, respectively: ISL width = 16.5 mm and 16.0 mm; SSL width = 4.3 mm and 3.8 mm; ISL + SSL area = 17.2 mm and 25.7 mm; these differences were not significant. Significant differences did exist in terms of spinous process angle *vs.* spine axis (47° for scoliosis and 32° for kyphosis) and SSL thickness (2.1 mm for scoliosis and 3.0 mm for kyphosis). Fourth-step median relaxation was 42% for scoliosis and 49% for kyphosis. Median linear region stiffness was 42 N/mm for scoliosis and 51 N/mm for kyphosis. Median failure load was 191 N for scoliotic and 175 N for kyphotic ligaments. Differences in loading, relaxation, viscoelastic and failure parameters were not statistically significant, except for a trend for greater initial rate of relaxation (T1) for scoliosis ligaments. However, we found significant morphological differences related to the spinous processes, which suggests a need for future biomechanical studies related to the musculoskeletal aspects of spinal alignment and posture.

1. Introduction

Idiopathic scoliosis and Scheuermann's kyphosis are developmental conditions leading to the deformity of the adolescent spine. Advanced cases of spinal deformity may require spinal fusion. While fusion usually arrests the progression of deformity, fusion also limits the flexibility of the spine and is attributed to degenerative changes of adjacent motion segments levels later in life. Because even the secondary biological and mechanical stages of these diseases are poorly understood, the development of targeted treatments remains difficult. Optimally, non-fusion treatment is desirable.

Scoliosis patients often have hypokyphotic thoracic spines relative to normal adolescent population (de Jonge et al., 2002). One may speculate that this is due to taut ligaments of the posterior elements in scoliosis patients relative to lax ligaments in Schuermann's patients. The authors have noted a qualitative relationship between spine deformity and quality of the supraspinous and interspinous ligaments (SSL and ISL, respectively) during surgical treatment. Specifically, the ISL and SSL in scoliotic patients appear thick and the spinous processes appear relatively perpendicular to the long axis of the spine. Conversely, the spinous processes in kyphotic subjects tend to be angled downward, and the ISL and SSL tend to appear thin and hypoplastic.

Quantifying such a relationship in these structures would demonstrate a correlation between biomechanical ligament properties and deformity. Though it is understood that such a link in itself cannot determine causation, establishing a connection between ligament properties and spinal deformity would identify a biological or mechanical connection that could be explored in future studies. Such studies might investigate causation through animal models, explore *in vivo* ligament differences using medical imaging, biochemical or histological analysis, improve mathematical models, or evaluate treatment by ligament modification or augmentation.

* Corresponding author. Tel.: +1 651 260 9887.
E-mail address: bpwbeaubien@gmail.com (B.P. Beaubien).

http://dx.doi.org/10.1016/j.jbiomech.2015.12.012
0021-9290/

To our knowledge, no comparative study has analyzed the SSL/ISL complex using rigorous biomechanical analysis techniques, and no study has biomechanically compared these ligaments as formed in the presence of scoliosis to those formed in the presence of kyphosis. A pilot study by the lead author investigated mechanical testing and analysis methods for the evaluation of posterior spinal ligaments in a porcine model. The goal of the present study was to apply these methods to the human SSL/ISL complex to describe possible differences in the viscoelastic properties between scoliotic and kyphotic patients. Although the SSL/ISL unit represents an inhomogenous and locally anisotropic tissue (Aspden et al., 1987), samples in this study were tested uni-axially in their natural configuration in order to compare these clinically obtained tissues, which act together *in vivo*.

On the basis of possible functional differences and visually observed differences, this study hypothesized that the ISL/SSL complexes would differ both morphologically and in terms of their mechanical performance. Evaluation of these hypotheses was performed by making *in vitro* and *in vivo* dimensional measurements, and by stress-relaxation testing and load-to-failure testing. Mechanical performance data were evaluated both in terms of structural performance (load–displacement) and material properties (stress–strain) to separate load response differences due to differing morphology.

2. Methods

2.1. Clinical measurements

Preoperative standing coronal and sagittal spinal radiographs were measured for each subject to determine the degree of their scoliosis and kyphosis. The Cobb method was used over the entire length of the curve and across the local curve (the region of the tissue specimens). MRIs from all patients were reviewed to confirm that there were no traumatic or congenital conditions. Axial images were measured to determine the size of the spinous process and the total transverse sagittal length of the vertebra. Axial images allow measurements to be obtained while taking into account axial rotation. Specifically, T2 weighted images were used for measurements after confirming that the images were parallel to the intervertebral disc and endplates. T1 weighted images were also used in 5 cases in which there was better delineation between the tissues at the anterior vertebral bodies. The transverse length of the spinous process was determined as the distance from the posterior margin of the canal to the posterior tip of the spinous process, and the vertebral length was determined as the distance from the anterior vertebral margin to the posterior tip of the process. Due to the caudal alignment of the spinous processes on a given axial image, the anterior reference point would usually be one vertebral level below the level of the posterior process measurement point. This required verification that there was no change in spinous process length from one vertebral level to the adjacent level being measured. The spinous process "Lever Arm" was the spinous process length measured at the tested level (apex of the spinal curve) from the spinous process–lamina junction to the tip of the spinous process in a direction perpendicular to the long axis of the corresponding motion segment. The vertebral body depth was measured along the same axis from the anterior margin to posterior margin of the vertebral body, Fig. 1.

2.2. Tissue procurement

After internal review board approval, 14 adolescent idiopathic scoliosis and 8 Scheuermann kyphosis patients undergoing posterior spinal surgery for treatment of their deformity had tissue excised at the apex of their curvature. The tissue obtained consisted of three to four adjacent spinous processes with intervening ligaments. The technique entailed scoring the junction of the base of the spinous process to laminar junction and then using small osteotomes or gouges in a direction tangential to the lamina to release the spinous processes from the laminae. Muscle and fascia were carefully removed from these specimens. The time from tissue harvest to freezing was less than 60 min. All tissue was double-wrapped in airtight plastic bags and frozen at -20 °Celsius (C), where it was stored until the time of testing.

2.3. Tissue preparation and measurement

Specimens were thawed, placed in 0.9% phosphate-buffered saline (PBS, Fisher Scientific, BP665-1), and refrigerated for approximately 24 h before testing.

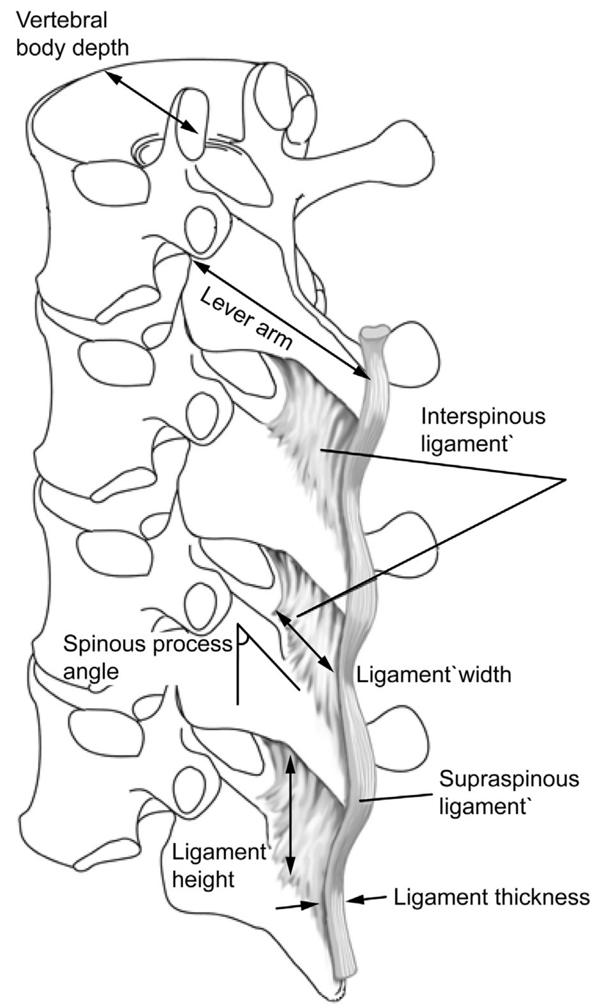

Fig. 1. Schematic identification of measured morphologic parameters.

Specimen width and thickness were measured using a digital caliper in the locations indicated in Fig. 1. Cross-sectional area was calculated assuming an elliptical cross-sectional shape for the supraspinous ligament, and a rectangular cross-sectional shape for the much wider interspinous ligament. Special grips, shown in Fig. 2, were designed to allow testing of the central level of multiple-level specimens. For a four-level specimen (*e.g.*, T7–T10), the outer levels (between T7 and T10) are fixed first, followed by the inner levels (between T8 and T9), which are fixed with the specimen under 1 N of applied axial loading for testing of the central ligament (*e.g.*, T8–T9). Pilot testing revealed the importance of measuring only the ligamentous region of the ISL when determining the initial length of the ligament, and so the interspinous process ligament length was measured on scaled fluoroscopic images acquired with the ligament under 1 N of axial tension, exclusive of the weight of the tissue. Ligament length was measured at three points across the spinous processes, and the average of these three points was used as the initial, unloaded length of the specimen.

2.4. Stress relaxation testing

In developing the mechanical test protocol, a balance was sought between minimal test time and rigorous description of the mechanical properties of the system. An incremental step relaxation protocol consisting of four stretch steps from 1.04 to 1.16 with a 1000-second relaxation period was chosen to evaluate viscoelastic properties (Fig. 3). The magnitude of this stretch is similar to that seen using *in vitro* flexibility tests (Panjabi et al., 1982) and is well below the estimated failure strain of these ligaments. The relaxation period was chosen as it allowed the load to approach equilibrium in pilot tests. A video strain measurement system was used during pilot testing, but it was found that surface strains did not necessarily correlate linearly with subsurface strains owing to the presence of a fine membrane on the surface of the ligaments. Furthermore, it was the net displacement of the spinous processes that was of the most interest clinically. For this reason, crosshead displacement was used to calculate the net stretch of the ligament.

Stress relaxation experiments were conducted in a PBS bath to ensure hydration and at body temperature (37 ± 1 °C). Displacements were applied to the bone–

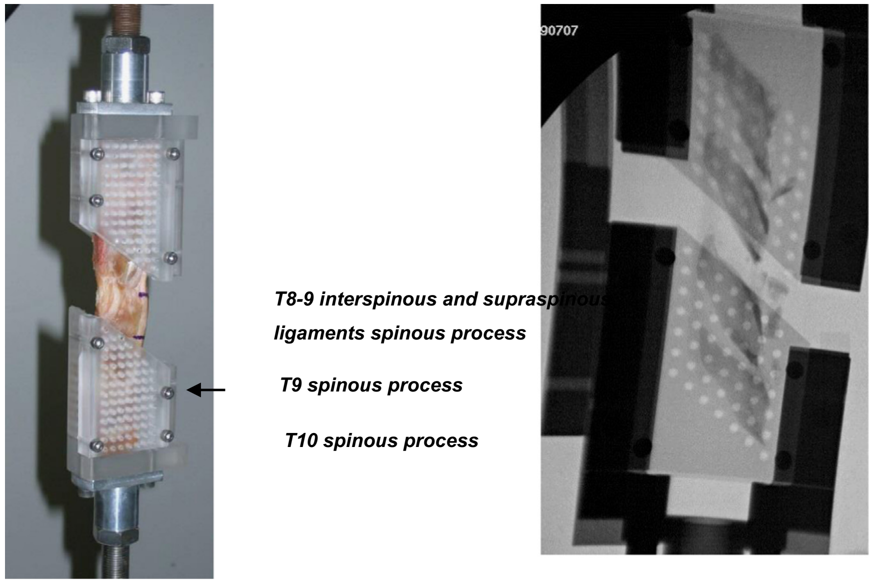

Fig. 2. Custom grips designed to allow immobilization of multiple spinous processes as shown in the photograph (left) and fluoroscopic image (right). Both images are in air prior to testing in saline.

ligament–bone specimens on a uni-axial materials testing machine (MTS 810 uni-axial loadframe, Minneapolis, MN), with a 100 lbf load cell).

A tensile preload of 1.0 N, exclusive of the weight of the tissue, was applied for 90 s prior to initiating each test. To obtain a consistent load response, two sets of preconditioning cycles were performed to the peak stretch level of 1.16: the first set consisted of 30 sinusoidal cycles and the second of 90 sinusoidal cycles, each at a frequency of 0.5 Hz. A recovery period equal to twice the duration of each preconditioning cycle was allowed before testing continued.

2.4. Data analysis

2.4.1. Stress relaxation testing

The stress relaxation data were evaluated in two steps. First, a nonlinear function was fit to the elastic loading portion of the experiment. The following exponential growth form of the nonlinearly elastic function has been widely applied and was used in this study (Fung, 1972) with the addition of the initial preload, F_0:

$$F(d) = A[e^{\beta d} - 1] + F_0 \tag{1}$$

where d is the applied displacement, F is the resultant load, and A and β are the linear and nonlinear components of the elasticity.

The relaxation data were fit next. The amount of load relaxation was calculated first as the percentage drop in load over a given step. Specifically,

$$R_i = (F_{i,s} - F_{i,e})/(F_{i,s})' \times 100\% \tag{2}$$

where $F_{i,s}$ and $F_{i,e}$ are the force at the start and end, respectively, of the current increment less the equilibrium force of the previous increment. Finally, the shape of the relaxation curve was fit by normalizing the load drop for each step and then fitting a Kelvin model to the normalized data. A single element model was initially used, but did not fit the data well, and so the following two-element model was fit to the data:

$$Q_i(t) = [G_1 e^{-t/\tau_1} + (1 - G_1) e^{-t/\tau_2}] \tag{3}$$

where Q_i is the normalized load for a given step, τ_1 and τ_2 are the long and short time constants, respectively, and G_1 and $1 - G_1$ are the weighting coefficients for these constants. The second weighting coefficient in this two element model, often represented by G_2 in Kelvin models, was substituted with $(1 - G_1)$ to fit these normalized data with fewer variables, thus making each fit more unique. Normalized data from all steps were used to perform the curve fits.

2.4.2. Failure testing

Stretch-to-failure testing was performed on each specimen after stress relaxation testing. A 1000 s recovery period was allowed under a 1 N tensile load prior to failure testing. Failure testing consisted of stretching specimens at a rate of 5 mm/min until failure while measuring the resultant load. Load–displacement curves were generated and the secant stiffness (i.e., the load displacement in the linear region of the curve) and peak load were calculated. Engineering modulus was calculated as the stiffness divided by the cross sectional area.

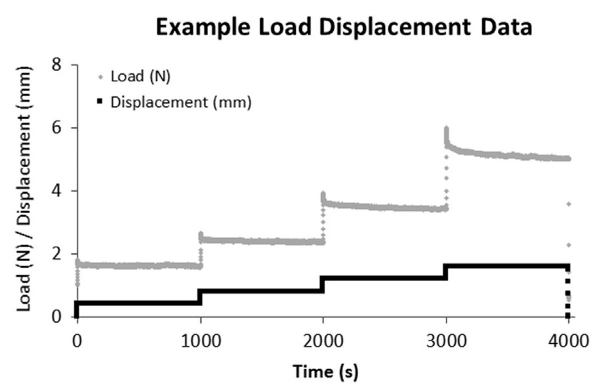

Fig. 3. Applied displacement and resulting load corresponding to the 1.04, 1.08, 1.12, and 1.16 stretch steps for a single specimen.

2.4.3. Statistics

Descriptive statistics were performed on all outcome measures and included median and interquartile ranges. The ligament parameters were tested for evidence of a statistical difference *via* a two-sided t-test using the Satterthwaite method, as the F test for equality of variance indicated unequal variances with $p < 0.05$. Additional analyses assessed for the presence of a difference in the ligament parameters by patient age, gender, and scoliosis or kyphosis degrees. For the continuous parameters, the test was evaluated for a correlation coefficient that did not equal 0, whereas for gender, the Wilcoxon nonparametric test was used. Correlation coefficients are given for continuous parameters showing statistical evidence of a correlation with age or radiographic scoliosis or kyphosis degrees over the entire curve. Differences were considered statistically significant for $p < 0.05$.

2. Results

Demographic data differed only in that 9 of 14 scoliosis subjects were females but only 1 of 8 kyphosis subjects were female. The scoliosis group had a median age of 17 years (range, 14–29 years), a median height of 167 cm (157–180 cm), a median weight of 57 kg (43–80 kg), and a body mass index of 21 kg/m^2 (17–28 kg/m^2). In the kyphosis group, the median age was 17 years (range, 15–20 years), the median height 175 cm (164–185 cm), the median weight 69 kg (58–109 kg), and the body mass index 22 kg/m^2 (20–35 kg/m^2).

Several morphometric differences were noted between scoliotic and kyphotic groups, as shown in Table 1. *In vivo* radiographs found the primary curve for the scoliosis patients was thoracic in all cases with the proximal vertebral level ranging from T4 to T6 and the distal level ranging from T11 to L2. The number of scoliotic levels were: 6 ($n=1$), 7 ($n=7$), 8 ($n=5$), and 10 ($n=1$).The apex of the scoliosis ranged from T8 to T10. The ligaments that were tested for the scoliotic patients ranged from T6 to T9 for the proximal level and T8 to T11 for the distal level. The kyphosis patients all had thoracic curve with the proximal vertebral level ranging from T1 to T3 and the distal level ranging from T12 to L3. The number of kyphotic levels were: 10 ($n=1$), 11 ($n=3$), 12 ($n=1$), 14 ($n=2$), and 15 ($n=1$).The apex of the kyphosis ranged from T6 to T10. The ligaments that were tested for the kyphotic patients ranged from T5 to T9 for the proximal level and T8 to T11 for the distal level. Cobb angle measures differed for the coronal spinal curvature, which was significantly greater for the scoliosis group, and sagittal spinal curvature, which was significantly greater for the kyphotic group (both $p<0.001$). These results held true for measurements made of specimen curvature over the region of the curve tested ($p<0.001$). *In vitro* measurements differed significantly in terms of SSL thickness, which was greater for the kyphosis group ($p=0.048$) and spinous process angle ($p<0.001$), which was greater for the kyphotic group ($p<0.002$). The spinous process lever arm tended to be smaller in the kyphotic group, but this difference did not reach statistical significance ($p=0.052$); however, when normalized to the vertebral body mid-sagittal width, this difference was statistically significant ($p<0.001$).

Neither stepwise relaxation data (Table 2) nor load-to-failure data (Table 3) demonstrated significant differences between kyphosis and scoliosis groups. In Figs. 4 and 5, curve fits are shown for the loading and relaxation portions of the tests, respectively. In the load-to-failure tests, failure occurred mid-substance in all specimens.

The scoliosis angle was weakly correlated with the SSL thickness ($r=-0.44$) but strongly correlated with the spinous process angle ($r=0.81$, $p<0.001$). The kyphosis angle was correlated most strongly with spinous process angle ($r=-0.74$, $p<0.001$), while ligament length and T1 also have a statistically significant, but weaker, association. A plot of spinous process angle *vs.* scoliosis angle and kyphosis angle is shown in Fig. 6.

3. Discussion

The present study found morphometric differences but no differences in intrinsic biomechanical properties of thoracic supra- and intraspinous ligament complexes between scoliosis and kyphosis patients. Literature values for ISL/SSL stiffness and failure parameters in the current study tended to be lower as compared to many studies but were in the range of others. One prior study of scoliosis patient ligaments found an ISL/SSL elastic modulus of 129 ± 42 MPa, which was substantially higher than that calculated from the load to failure data in this study (Waters and Morris, 1973). This prior study did not find a difference in modulus of adolescent idiopathic scoliosis relative to other scoliosis types. Another prior study of normal lumbar ISL and SSL specimens found elastic modulus values of 24 ± 11 MPa (Pintar et al, 1992), which is comparable to the current study. In two other studies, stiffness of normal ISL/SSL complexes was calculated to be 134 ± 26 N/mm (Dumas et al., 1987), and peak loads and displacements were 187 ± 106 N and 3.7 ± 1.5 mm, respectively (Chazal et al., 1985). The difference in modulus values between studies may be due in part to the loading rates or area measurement methods. Failure values may have also differed among studies in part because the ligaments in the current study were exposed to relaxation testing before failure testing, which may have resulted in some subfailure damage. Despite these noted differences, within-study comparisons are still considered relevant.

Whereas previous studies on normal interspinous and supraspinous ligaments have evaluated only load to failure data, the current study also evaluated their viscoelastic behavior. Stress relaxation tests were performed over 4 steps, and data were evaluated by calculating percent relaxation, and fitting nonlinear loading and relaxation parameters utilizing a 3 variable model. This model fit the data well, but did not detect any statistically significant differences in the ligaments between kyphotic and scoliotic patients. Due to the lack of existing relaxation test data on normal interspinous and supraspinous ligaments, these viscoelastic parameters can only be compared within-study for the ligaments that were excised and tested.

Morphological differences between scoliosis and kyphosis patients included both the spinous process angle, and the spinous process length, or “Lever Arm” (sagittal width). In kyphotic patients, spinous process angle in the sagittal plane was significantly more acute, and the Lever Arm was significantly lower. This confirms the hypothesis and clinical observation that spinous processes are angled caudally and have a lower profile in kyphosis as compared to scoliosis patients. Bony morphological differences between scoliosis and kyphosis patients have previously been described, such as coronal vertebral body wedging for scoliosis vs sagittal wedging for kyphosis patients (Parent et al., 2002; Stokes and Aronsson, 2001). Furthermore, posterior element coronal asymmetrical morphology has been described for scoliosis (Liljenqvist et al., 2000; Parent et al., 2002).

Table 1
Median (interquartile range) measurements from *in vivo* imaging and laboratory measurements.

		Scoliosis	Kyphosis	p
Radiographic	Scoliosis curve (entire, deg)	48 (45–50)	8 (0–19)	< 0.001
	Kyphosis curve (entire, deg)	23 (13–28)	77 (74–83)	< 0.001
	Scoliosis curve (local, deg)	32 (27–39)	4 (2–7)	< 0.001
	Kyphosis curve (local, deg)	7 (2–14)	41 (37–49)	< 0.001
	Lever Arm (mm)	20 (18.3–21.5)	17.5 (15.8–18.5)	0.052
	Lever arm, normalized[a]	1.00 (0.94 – 1.2)	0.60 (0.51 – 0.67)	< 0.001
In vitro	ISL thickness (mm)	0.5 (0.5–0.6)	0.8 (0.5–1.5)	0.18[a]
	ISL width (mm)	16.5 (15.0–19.8)	17.0 (15.0–17.6)	0.19[a]
	SSL thickness (mm)	2.1 (2.0–2.4)	3.0 (2.5–3.5)	0.048
	SSL width (mm)	4.3 (3.1–5.0)	4.0 (3.3.–4.9)	0.58
	Total area (mm^2)	17.2 (15.0–21.4)	21.9 (18.0–30.3)	0.18
	SP angle	47 (43–48)	32 (26–37)	< 0.001
	Loaded length (mm)	9.3 (7.6–10.0)	9.8 (8.8–13.9)	0.25[a]

[a] Lever arm normalized to the vertebral body depth.

Table 2
Loading and step relaxation results.

		Scoliosis			Kyphosis		
		Median	*1st quartile*	*3rd quartile*	*Median*	*1st quartile*	*3rd quartile*
Loading	*A*	2.08	1.42	3.54	1.86	1.19	2.96
	B	1.09	0.91	1.40	1.36	0.92	1.57
Relaxation	*Relaxation (step 1)*	37%	28%	44%	33%	16%	39%
	Relaxation (step 2)	41%	28%	47%	41%	25%	49%
	Relaxation (step 3)	40%	33%	47%	44%	26%	52%
	Relaxation (step 4)% Relax	42%	37%	52%	50%	47%	56%
	G1	0.62	0.58	0.67	0.66	0.60	0.67
	1 – G1	0.38	NA	NA	0.34	NA	NA
	T1	4.1	2.8	5.0	3.3	2.95	4.2
	T2	288	247	305	305	296.7	327

Table 3
Median (interquartile range) failure parameters.

	Linear region stiffness (N/mm)	Modulus of elasticity (MPa)	Ultimate Failure Load (N)	Failure stress (MPa)
Scoliosis	42 (28–81)	19 (15–38)	191 (109–220)	7 (5–11)
Kyphosis	61 (38–81)	16 (13–38)	189 (126–237)	9 (3–11)

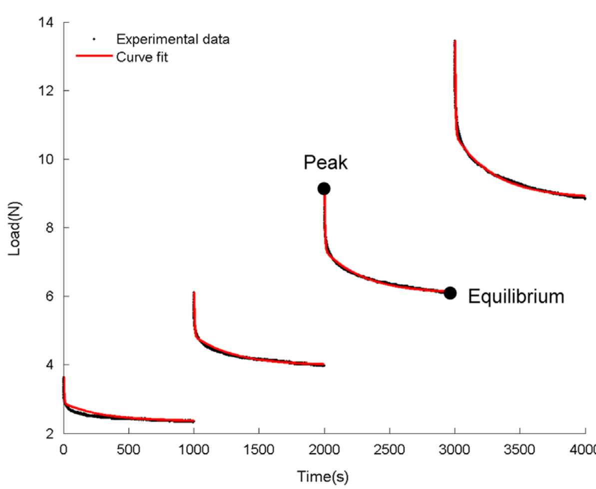

Fig. 4. Example relaxation data (red) and curve fit (black). Each step was first normalized to its peak value, and the curve fit was applied to the normalized data. Peak and equilibrium values are identified on this graph for the third loading step. (For interpretation of the references to color in this figure legend, the reader is referred to the web version of this article.)

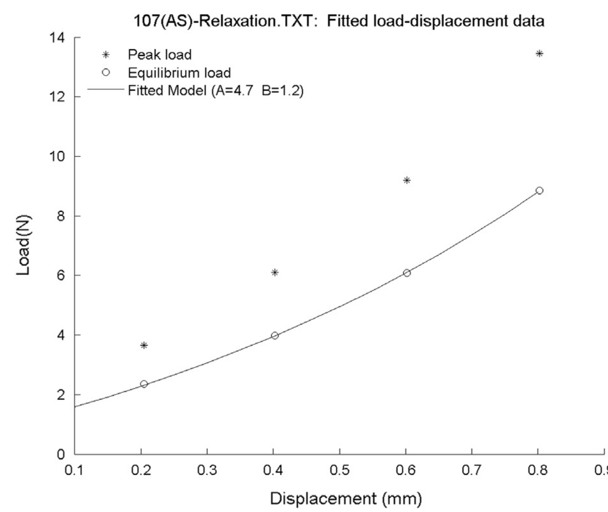

Fig. 5. Example curve showing a fit of the equilibrium load data from the incremental step relaxation test.

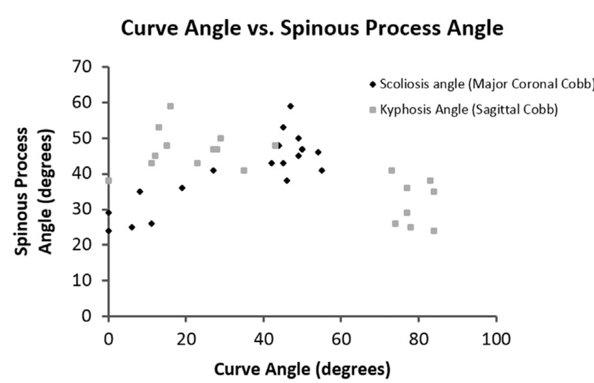

Fig. 6. Spinous process angle at various degrees of spinal angle. All data are shown from both scoliotic and kyphotic groups (i.e., the kyphosis angle is the sagittal Cobb angle from all patients in the kyphotic and scoliotic groups).

Differences in the kyphotic angle and "Lever Arm" of the spinous process between groups may relate to the mode of engagement of the ligaments. As the spinal segments flex and extend, the supraspinous and interspinous ligaments are stretched proportionally to their distance from the center of rotation of the spinal segment, which is typically near the posterior margin of the vertebral body for flexion / extension motions (White and Panjabi, 1990). Whereas the ligaments from kyphotic and scoliotic patients tested in this study provided a similar load response at a given elongation, kyphotic group ligaments had shorter normalized spinous process lengths. Resistance to a given flexion moment, such as an individual with kyphosis and short spinous processes holding heavy objects in front of them, would therefore place greater stress on these ligaments. One may speculate that this increased stress would lead to additional ligament creep and elongation over time, and thus an even more kyphotic spine. It should be noted that the actual axis of rotation and lever arm were not measured in this study, and instead the lever arm was represented as the spinous process sagittal width. Future studies might focus on *in vivo* or *in vitro* analyses specifically focusing on the nature of this relationship, load-sharing with spinal musculature, or histological properties of the ligaments to better describe this relationship.

It is currently believed that the primary function of the ISL is to resist excessive flexion loads (Hindle et al., 1990). Clinical studies have found mechanical damage to the ISL after surgical destabilization, destabilizing spinal disease (Fujiwara et al., 2000), or other physical trauma. Integrity of ISL and SSL may be important in preventing kyphosis and instability as has been demonstrated in trauma cases. Another clinical entity, “proximal junctional kyphosis,” relates to kyphosis directly above a spinal fusion construct and may be related to injury to the SSL/ISL complex. Biomechanical studies have noted the importance of preserving the SSL/ISL complex to avoid adjacent segment kyphosis and maintaining motion segment flexion stiffness (Anderson et al., 2009; Cahill et al., 2012; Kretzer et al., 2010; Aubin et al., 2015).

Other biomechanical studies have also suggested that weakening of the interspinous or supraspinous ligaments may lead to kyphotic deformity (Heuer et al., 2007). Static flexion loads are primarily resisted by the posterior structures including, in order of the degree of restriction, the ligamentum flavum, the articular ligaments, the ISL and the SSL (Dumas et al., 1987). Substantial strains are experienced by the most posterior ligaments, and *in situ* studies found that at an applied moment of 15 Nm the ISL and SSL experience mean strains of 17% and 18%, respectively (Panjabi et al., 1982).

Limitations of this study include a small sample size, repeated testing on the same specimens, and the fact that the supraspinous ligament is not directly gripped in the fixture during testing. There was also a disparity in the magnitude of ligament stiffness between this and prior studies, possibly owing to fixture or test methods. Only mechanical testing was performed, and as such possible histologic or biochemical differences between groups were not evaluated. A general limitation is that this study is not comprehensive and did not address the potential *in vivo* ability of posterior muscles to resist flexion loading. Finally, ligaments did not relax to equilibrium, despite the fact that pilot testing in porcine specimens appeared approach equilibrium under the same protocol. While it is recommended that future studies test for a longer duration, data from the model fit the existing curve well and did not assume equilibrium was reached. Notwithstanding these limitations, the results of this study are assumed to be relevant comparisons across groups.

In conclusion, intrinsic SSL/ISL complex viscoelasticity was generally similar for scoliosis and kyphosis, but significant morphological differences related to the spinous processes exist. The observation of these differences indicates a direction for future study related to the musculoskeletal aspects of spinal alignment and posture.

Conflict of interest statement

This basic research was supported by the senior author. There are no conflicts of interest with any authors.

Acknowledgments

All authors were fully involved in the study and preparation of the manuscript. The material within has not been and will not be submitted for publication elsewhere. The authors would like to thank Drs. Jack Lewis, Victor Barocas and Susan Mantell of the University of Minnesota for their advisory assistance in study design and data analysis. All funding was provided by the senior author.

References

Anderson, A.L., McIff, T.E., Asher, M.A., Burton, D.C., Glattes, R.C., 2009. The effect of posterior thoracic spine anatomical structures on motion segment flexion stiffness. Spine 34 (5), 441–446.
Aspden, R.M., Bornstein, N.H., Hukins, D.W., 1987. Collagen organisation in the interspinous ligament and its relationship to tissue function. J. Anat. 155, 141–151.
Aubin, C.E., Cammarata, M., Xiaoyu, W., Mac-Thiong, J.M., 2015. Instrumentation strategies to reduce the risks of proximal junctional kyphosis in adult scoliosis: a detailed biomechanical analysis. Spine Deform. 3 (3), 211–218.
Cahill., P.J., Wang, W., Asghar, J., Booker, R., Betz, R.R., Ramsey, C., Baran, G., 2012. The use of a transition rod may prevent proximal junctional kyphosis in the thoracic spine after scoliosis surgery: a finite element analysis. Spine 37 (12), E687–E695.
Chazal, J., Tanguy, A., Bourges, M., Gaurel, G., Escande, G., Guillot, M., Vanneuville, G., 1985. Biomechanical properties of spinal ligaments and a histological study of the supraspinal ligament in traction. J. Biomech. 18, 167–176.
de Jonge, T., Dubousset, J.F., Illés, T., 2002. Sagittal plane correction in idiopathic scoliosis. Spine 27 (7), 754–760.
Dumas, G.A., Beaudoin, L., Drouin, G., 1987. In situ mechanical behavior of posterior spinal ligaments in the lumbar region: an in vitro study. J. Biomech. 20 (3), 301–310.
Fung, Y.C., 1972. Stress strain history relations of soft tissues in simple elongation. In: Fung, Y.C., Perrone, N., Anliker, M. (Eds.), Biomechanics, its Foundations and Objectives. Prentice Hall, Englewood Cliffs, NJ.
Fujiwara, A.F., Tamai, K.F., An, H.S., Shimizu, K.F., Yoshida, H.F., Saotome, K., 2000. The interspinous ligament of the lumbar spine. Magnetic resonance images and their clinical significance. Spine 25 (3), 358–363.
Heuer, F., Schmidt, H., Klezl, Z., Claes, L., Wilke, H.J., 2007. Stepwise reduction of functional spinal structures increase range of motion and change lordosis angle. J. Biomech. 40 (2), 271–280.
Hindle, R.J., Pearcy, M.J., Cross, A., 1990. Mechanical function of the human lumbar interspinous and supraspinous ligaments. J. Biomed. Eng. 12 (4), 340–344.
Kretzer, R.M., Hu, N., Umekoji, H., Sciubba, D.M., Jallo, G.I., McAfee, P.C., Tortolani, P. J., Cunningham, B.W., 2010. The effect of spinal instrumentation on kinematics at the cervicothoracic junction: emphasis on soft-tissue response in an in vitro human cadaveric model. J. Neurosurg. Spine 13 (4), 435–442.
Liljenqvist, U.R., Link, T.M., Halm, H.F., 2000. Morphometric analysis of thoracic and lumbar vertebrae in idiopathic scoliosis. Spine 25 (10), 1247–1253.
Panjabi, M.M., Goel, V.K., Takata, K., 1982. Physiologic strains in the lumbar spinal segments: an *in vitro* biomechanical study. Spine 7 (3), 192–203.
Parent, S., Labelle, H., Skalli, W., Latimer, B., de Guise, J., 2002. Morphometric analysis of anatomic scoliotic specimens. Spine 27 (21), 2305–2311.
Pintar, F.A., Yoganandan, N., Myers, T., Elhagediab, A., Sances Jr., A., 1992. Biomechanical properties of human lumbar spine ligaments. J. Biomech. 25, 1351–1356.
Stokes, I.A., Aronsson, D.D., 2001. Disc and vertebral wedging in patients with progressive scoliosis. J. Spinal Disord. 14 (4), 317–322.
Waters, R.L., Morris, J.M., 1973. An in vitro study of normal and scoliotic interspinous ligaments. J. Biomech. 6, 343–348.
White, A., Panjabi, M., 1990. Clinical Biomechanics of the Spine, Second Edition Lippincott Williams & Wilkins, Philadelphia, PA.